Liquid Crystals
Publication details, including instructions for authors and subscription information:
http://www.informaworld.com/smpp/title~content=t713926090

Synthesis and mesomorphic properties of compounds exhibiting the undulated twist grain boundary smectic C* phase

S. Shubashree[a]; B. K. Sadashiva Corresponding author[a]
[a] Raman Research Institute, Bangalore 560 080, India

Online publication date: 19 May 2010

To cite this Article Shubashree, S. and Sadashiva Corresponding author, B. K.(2004) 'Synthesis and mesomorphic properties of compounds exhibiting the undulated twist grain boundary smectic C* phase', Liquid Crystals, 31: 1, 81 — 89
To link to this Article: DOI: 10.1080/02678290410001643953
URL: http://dx.doi.org/10.1080/02678290410001643953

LIQUID CRYSTALS, VOL. 31, NO. 1, JANUARY 2004, 81–89

Synthesis and mesomorphic properties of compounds exhibiting the undulated twist grain boundary smectic C* phase

S. SHUBASHREE and B. K. SADASHIVA*

Raman Research Institute, C.V. Raman Avenue, Sadashivanagar, Bangalore 560 080, India

(*Received 22 July 2003; accepted 19 August 2003*)

The synthesis and characterization of three homologous series of compounds exhibiting the undulated twist grain boundary smectic C* ($UTGB_{C*}$) phase are reported. The chiral mesophases have been obtained using cholesterol as the chiral moiety. Cholestanol and [*S*]-[+]-octan-2-ol have also been used as the chiral moiety for comparitive purposes. In addition to this novel phase, cholesteric, smectic A, smectic C* and TGB_A phases have also been observed. The mesophases were characterized using a combination of polarizing optical microscopy, differential scanning calorimetry, X-ray diffraction and measurement of helical pitch.

1. Introduction

Since the discovery of the liquid crystalline state in cholesteryl benzoate [1], chirality in liquid crystal systems has played a major role in the development of new materials with new mesomorphic properties. In this regard, the discovery of ferroelectricity in chiral liquid crystals in 1975 is a very important contribution [2]. A little later the first antiferroelectric liquid crystal phase was observed while studying the electro-optical behaviour in a chiral compound, namely 4-(1-methylheptyloxycarbonyl)phenyl 4′-octyloxybiphenyl-4-carboxylate [3]. Around the same time, the twist grain boundary (TGB) phase consisting of chiral molecules and theoretically predicted by Renn and Lubensky [4] was discovered by Goodby *et al.* [5, 6]. The TGB phase is characterized as having smectic layers, with blocks of these rotating to produce a helical structure. Depending on the local smectic order, three types of TGB phases were theoretically predicted, namely, TGB_A, TGB_C and TGB_{C*} phases [7], and the first two phases have been observed in a number of compounds.

More recently, Pramod *et al.* [8] discovered a new TGB phase in a binary mixture of compounds whose structure is very different from those of the other known TGB phases. They called this new phase the undulated twist grain boundary smectic C* ($UTGB_{C*}$) phase. Based on a range of measurements including optical diffraction, X-ray diffraction and electro-optical experiments, they proposed a model for this new phase. According to their model, this phase is TGB_{C*} in nature, wherein there is a helical arrangement of tilted molecules within each SmC*-like block. In addition, there is a two-dimensional undulation of the SmC*-like blocks in the form of a square lattice. Thus, this three-dimensionally modulated structure has twist distortions along three mutually orthogonal directions. None of the previously proposed theoretical models anticipated such a structure with the undulating grain boundaries. Since this new phase was first discovered in a binary mixture of compounds, it was of obvious interest to obtain this novel phase in pure compounds. In view of this we carried out the synthesis of the following three series of compounds which represent the first example [9] of single component systems exhibiting the $UTGB_{C*}$ phase:

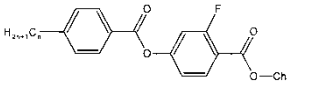

Series I $n = 8,9,10,11,12,14,16,18$

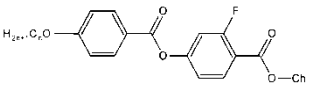

Series II $n = 9,10,11,12,14,16,18$

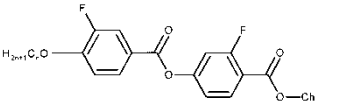

Series III $n = 7,8,9,10,11,12,14,16,18$

Ch = Cholesteryl moiety

*Author for correspondence; e-mail: sadashiv@rri.res.in

Liquid Crystals ISSN 0267-8292 print/ISSN 1366-5855 online © 2004 Taylor & Francis Ltd
http://www.tandf.co.uk/journals
DOI: 10.1080/02678290410001643953

2. Experimental

2.1. *Synthesis*

The 24 compounds belonging to the three homologous series of compounds I, II and III were synthesized following the general synthetic pathway shown in figure 1. The chiral moieties, cholesterol, cholestanol and [*S*]-[+]-octan-2-ol were all commercial products and used without further purification. The 4-*n*-alkyl- [10], 4-*n*-alkoxyl- [11] and 3-fluoro-4-*n*-alkoxyl-benzoic acids [12] were prepared following standard procedures. 2-Fluoro-4-benzyloxybenzoic acid was prepared according to a procedure already described [13, 14]. The procedure for the synthesis and characterization of compound **13** is given below.

2.1.1. *Cholesteryl 2-fluoro-4-(4-n-tetradecylbenzoyloxy)benzoate,* ***13***

A mixture of 4-*n*-tetradecylbenzoic acid (0.082 g, 0.26 mmol), cholesteryl 2-fluoro-4-hydroxybenzoate (0.15 g, 0.29 mmol), 4-(dimethylamino)pyridine (0.003 g, 0.025 mmol) and dry dichloromethane (5 ml) was stirred for 5 min. To this mixture was added 4-*N*,*N*-dicyclohexylcarbodiimide (0.059 g, 0.29 mmol) and stirring continued overnight at room temperature. The dicyclohexyl urea formed was filtered off and the filtrate diluted with dichloromethane (20 ml). The resultant solution was washed with 5% aqueous acetic acid (3×30 ml), water (3×50 ml), and dried over anhydrous sodium sulphate. The residue obtained on removal of solvent was chromatographed on silica gel and eluted with a mixture of chloroform and petroleum ether to yield the required compound as a white material. This was further purified by repeated crystallization from butan-2-one; yield 0.18 g, m.p. 99.5°C; $[\alpha]_D^{25} = 3.0^\circ$ $(10\,\mathrm{mgm\,ml^{-1}})$; ν_{max} (nujol); 2950, 1735, 1700, 1460, 1290, 1250 and 1050 $\mathrm{cm^{-1}}$; ^{1}H NMR ($CDCl_3$, 400 MHz) δ (ppm): 1.08–2.16 (m, 50H, $22 \times CH_2$–, $6 \times$ CH), 0.68 (s, 3H, tertiary CH_3), 1.06 (s, 3H tertiary CH_3), 0.855–0.87 [(d, 3H) and 0.859, 0.876 (d, 3H) $RCH(CH_3)_2$], 0.89–0.93 (m, 6H, $2 \times CH_3$), 2.46–2.48(m, 2H, allylic H), 5.42 (m, 1H, olefinic H), 2.6–2.7 (t, 2H, $ArCH_2$–), 4.86–5.0 (m, 1H, –CHOCOAr), 7.0–8.0 (m, 7H, ArH).

In general, the purity of all the compounds was checked by thin layer chromatography (Merck Kieselgel $60F_{254}$ pre-coated plates). The chemical structure of all the compounds was confirmed by ^{1}H NMR spectroscopy (Bruker AMX 400 spectrometer with 1% tetramethylsilane in deuteriochloroform as an internal standard) and infrared spectroscopy (Shimadzu FTIR-8400 spectrophotometer). Specific optical rotations were measured using chloroform as a solvent (Optical Activity AA1000 polarimeter).

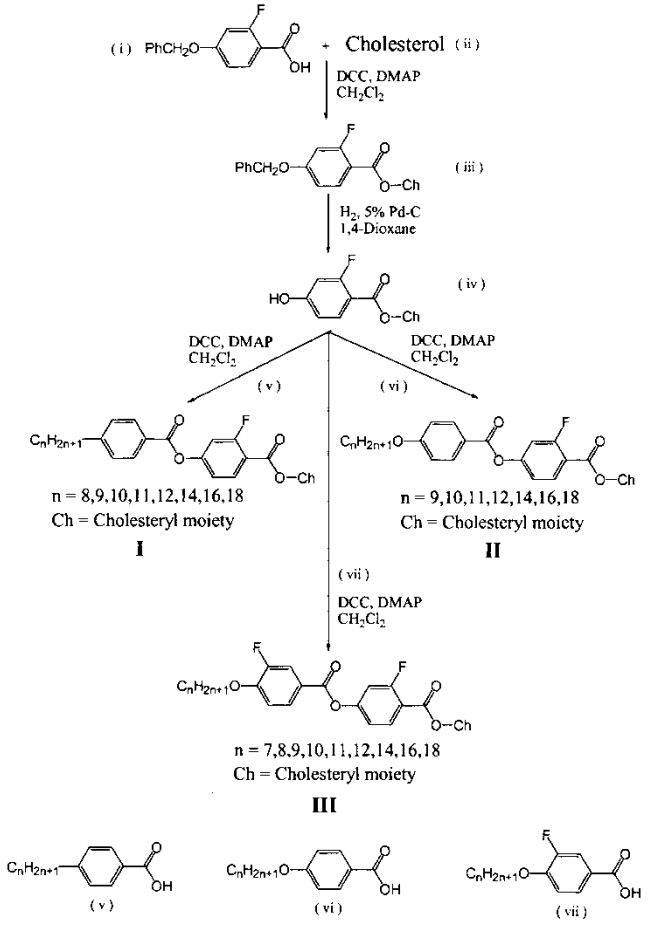

Figure 1. General synthetic scheme for the preparation of compounds of series I, II and III.

2.2. *Characterization*

The optical textures of the mesophases were examined using a polarizing microscope (Leitz Laborlux 12 POL) in conjunction with a heating stage and controller (Mettler FP 52 and FP5 control unit). The transition temperatures and associated enthalpy values were determined using a differential scanning calorimeter (DSC, Perkin-Elmer, Pyris 1D) operated at a scanning rate of $5^\circ\mathrm{C\,min^{-1}}$, both on heating and cooling cycles. The calorimeter was calibrated using indium as a standard. Helical pitch measurements were performed by the well known Grandjean–Cano method [15, 16]. The sample was taken in a low angle ($\approx 0.5^\circ$) wedge-shaped cell treated for planar alignment, constructed by using a mylar spacer of appropriate thickness (50 μm) at one edge of the cell. The helical pitch was determined by measuring the distance between the Grandjean–Cano lines as a function of temperature using a graduated eye-piece, which was calibrated using a

Table 1. Transition temperatures (°C) and enthalpies (kJ mol^{-1}) (in italics) for compounds of series I; ( ) indicates a monotropic transition. Cr = crystalline phase; SmC* = ferroelectric phase; SmA = smectic A phase; UTGB$_{C*}$ = undulated twist grain boundary smectic C* phase; TGB$_A$ = twist grain boundary smectic A phase; N* = cholesteric phase; d = decomposes.

Compound	*n*	Cr		SmC*		UTGB$_{C*}$		N*	
1	8	•	117.5 *43.3*	—		—		•	>230 d
2	9	•	119.5 *26.7*	•	(94.0) *0.28*	—		•	>230 d
3	10	•	117.0 *26.4*	•	(116.0) *0.24*	—		•	>230 d
4	11	•	116.5 *25.6*	•	124.0[a]	•	133.0 *0.19*	•	>230 d
5	12	•	111.0 *24.4*	•	144.0[a]	•	146.5 *0.23*	•	>230 d
6	14	•	99.5 *37.8*[b]	•	158.5[a]	•	164.0 *0.13*	•	>230 d
7	16	•	102.5 *29.0*	—	170.5[a]	•	177.5 *0.05*	•	>230 d
8	18	•	100.0 *30.4*	—	177.0[a]	•	185.0 *−0.19*	•	>230 d

[a]The enthalpy could not be measured.
[b]Total enthalpy including any other crystal–crystal transition.

micrometer scale provided by Leitz. X-ray diffraction (XRD) studies were carried out using CuK$_\alpha$ radiation from a rotating anode generator (Rigaku Ultrax-18) with a flat graphite crystal monochromator. The diffraction patterns were collected on an image plate (Marresearch). Unoriented samples were taken in Lindemann capillaries and the temperature was controlled to better than ±0.5°C.

3. Results and discussion

3.1. *Phase characterization and mesomorphic properties*

All the compounds synthesized were studied using polarizing optical microscopy and DSC. The transition temperatures and associated enthalpies for the three series I, II and III are summarized in tables 1, 2 and 3, respectively. All the compounds are mesomorphic and have very high clearing temperatures. However, they decompose when heated to beyond 230°C.

Compounds of series I show the following mesophases. For the shortest homologue (compound **1**), only a N* phase was observed which was identified from its characteristic platelet texture. Compounds **2** and **3** showed a monotropic SmC* phase in addition, with a schlieren texture. Compounds **4** to **8** are trimesomorphic and exhibit an interesting mesophase between the N* and SmC* phases. For example, compound **8**, in cells treated for homogeneous alignment, exhibits a planar texture at a high temperature of

Table 2. Transition temperatures (°C) and enthalpies (kJ mol^{-1}) (in italics) for compounds of series II: for key see table 1.

Compound	*n*	Cr		SmC*		UTGB$_{C*}$		N*	
9	9	•	112.0 *45.4*[b]	•	(99.0) *0.36*	—		•	>230 d
10	10	•	83.0 *34.1*	•	118.0 *0.27*	—		•	>230 d
11	11	•	94.5 *27.2*	•	128.0[a]	•	135.5 *0.29*	•	>230 d
12	12	•	111.0 *26.4*	•	132.5[a]	•	146.5 *0.21*	•	>230 d
13	14	•	85.5 *27.2*	•	163.0[a]	•	172.0 *0.35*	•	>230 d
14	16	•	102.0 *28.1*	•	175.5[a]	•	184.0 *0.24*	•	>230 d
15	18	•	86.0 *27.8*	•	181.5[a]	•	189.0 †	•	>230 d

[a]The enthalpy could not be measured.
[b]Total enthalpy including any other crystal–crystal transition.

Table 3. Transition temperatures (°C) and enthalpies (kJ mol^{-1}) (in italics) for compounds of series III: for key see table 1.

Compound	n	Cr		SmC*		SmA		$UTGB_{C*}$		TGB_A		N*	
16	7	•	141.0 *42.7*[b]	—		—		—		—		•	>230 d
17	8	•	115.0 *23.5*	•	121.0[a]	—		•	127.0 *0.26*	—		•	>230 d
18	9	•	115.5 *28.8*[b]	•	141.0[a]	—		•	149.5 *0.25*	—		•	>230 d
19	10	•	101.0 *22.4*	•	155.0[a]	—		•	165.0 *0.34*	—		•	>230 d
20	11	•	107.0 *33.8*[b]	•	168.0[a]	—		•	178.5 *0.50*	—		•	>230 d
21	12	•	110.0 *70.5*[b]	•	176.5[a]	—		•	186.0 *0.50*	—		•	>230 d
22	14	•	113.0 *31.8*	•	191.0[a]	—		•	199.0 *0.10*	—		•	>230 d
23	16	•	100.5 *33.7*	•	195.0[a]	—		•	196.0[a]	•	207.0[a]	•	>230 d
24	18	•	103.0 *36.4*	•	193.0[a]	•	209.5[a]	—		•	212.5[a]	•	>230 d

[a]The enthalpy could not be measured.
[b]Total enthalpy including any other crystal–crystal transition.

200°C, which is typical for a N* phase. In such samples the twist axis of the N* phase lies perpendicular to the surface of the glass plates. As the temperature was reduced, the planar texture of the N* phase changed to a well aligned square grid pattern. A photomicrograph of a typical square grid pattern obtained for this compound is shown in figure 2. This pattern is probably a consequence of the two-dimensional undulation of the TGB_{C*}-like blocks. This pattern is identical to the one observed for the $UTGB_{C*}$ phase discovered in mixtures [8]. On further cooling, a transition takes place to the SmC* phase, wherein the square grid pattern becomes hazy with different domains appearing in various colours. A slight shearing of the glass plates removed the square grid pattern completely which reappeared on heating the sample. The pseudo-homeotropic schlieren texture obtained on shearing the sample clearly indicates that this phase is SmC*.

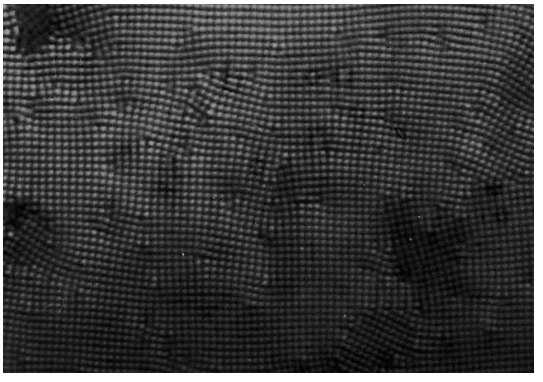

Figure 2. Photomicrograph showing the square grid pattern of the $UTGB_{C*}$ phase of a homogeneously aligned sample of compound **8** at 178°C.

It is known that in smectic phases molecular chirality can lead to the appearance of different types of long range director-modulated structures [17]. The existence of a phase with the periodic director rotation inside the smectic layer has been theoretically predicted [18–20]; it is believed to be associated with a regular array of defects. Different types of one and two-dimensional periodic system of defects were detected in freely suspended films of SmC* materials [17], which can lead to textures having periodic stripes or a square grid pattern. The appearance of a square grid pattern in SmC* phase is an interesting manifestation of molecular chirality.

In order to confirm that the square grid pattern seen in all the four compounds **4** to **8**, is not due to some instability in the SmC* phase, the samples were examined in wedge-shaped cells of appropriate thickness ($\sim$50 μm). In such cells, where the thickness varies continuously from one edge of the cell to the other, an array of equidistant Grandjean–Cano (GC) lines formed in the N* phase and a photomicrograph of this is shown in figure 3. The texture between the GC lines was smooth with gradual variation from the thinner to the thicker side of the cell. The colour variation was due to the change in the helical pitch induced by the treated glass plates. As the temperature was reduced, the square grid pattern appeared from the thinner side of each GC line and filled the entire field of view. The array of GC lines continued to exist and the spacing between them increased with decreasing

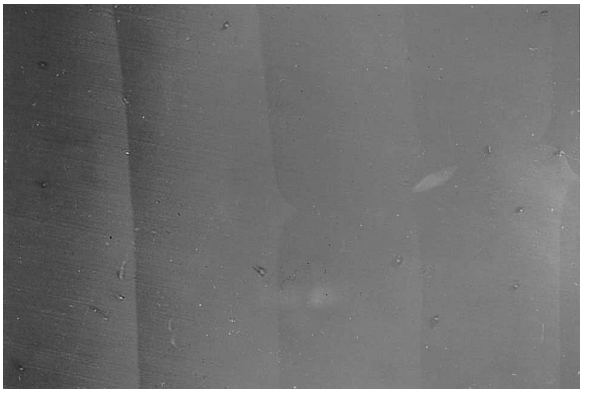

Figure 3. Photomicrograph of the Grandjean–Cano lines formed in the N* phase of compound **11** at 134°C.

temperature; when the transition took place to the SmC* phase, the GC lines became highly distorted and non-periodic. A photomicrograph of the square grid pattern of this intermediate phase in a wedge-shaped cell is shown in figure 4.

When compound **15** was observed in a cell treated for homeotropic alignment (with octadecyltriethoxysilane), a pseudo-homeotropic or a schlieren texture was observed (154.8°C), which is characteristic of a SmC* phase. On increasing the temperature further, bright corrugated filaments appeared with the tips of these filaments spiralling and continued to grow. A photomicrograph of the spiralling corrugated filaments is shown in figure 5. Near the transition to the higher temperature N* phase, the filaments coalesce ultimately to give rise to a platelet texture. All these observations, clearly indicate that the mesophase appearing between the N* and SmC* phases is indeed the undulated twist grain boundary smectic C* (UTGB$_{C*}$) phase. A plot of the transition temperatures as a function of the terminal *n*-alkyl chain length for compounds of series I is shown in figure 6.

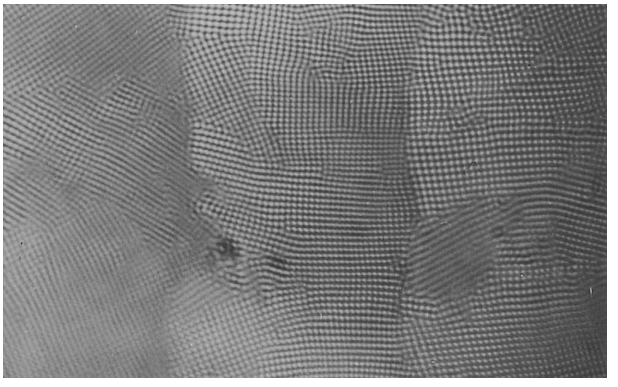

Figure 4. Photomicrograph of the square grid pattern of the UTGB$_{C*}$ phase seen in a wedge-shaped cell of compound **11** at 132°C.

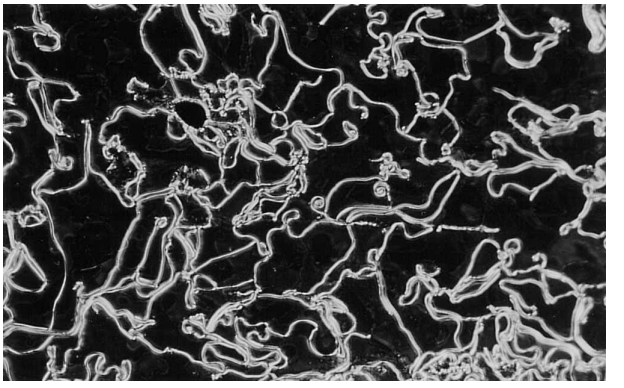

Figure 5. Photomicrograph of the UTGB$_{C*}$ phase showing the spiralling of the filaments, compound **15**.

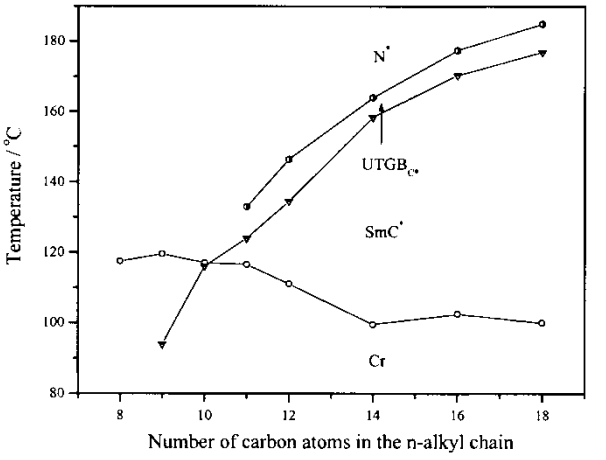

Figure 6. Plot of transition temperature versus the number of carbon atoms in the *n*-alkyl chain for series I.

In the case of compounds of series II which contain a terminal *n*-alkoxy chain (compounds **9** to **15**), the phase behaviour and sequences are similar to those observed in series I. However, in series III, where a fluorine substituent is introduced *ortho* to the terminal *n*-alkoxy chain, additional mesophases are induced. For example, compound **16** is monomesomorphic and exhibits only a N* phase. Compounds **17** to **22** exhibit N*, UTGB$_{C*}$ and SmC* phases, obtained also in the previous two series of compounds. Interestingly compound **23** shows N*, TGB$_A$, UTGB$_{C*}$ and SmC* phases on cooling from about 220°C. In the TGB$_A$ phase, the filaments are smooth but when the transition to a lower temperature phase takes place, the filaments become corrugated and also spiral at the tips. These features could be observed even though the thermal range of the mesophase is only 1°C. Surprisingly, for compound **24** the UTGB$_{C*}$ phase is eliminated and a SmA phase appears but the N*, TGB$_A$ and SmC* phases are retained. A plot of transition temperature *versus*

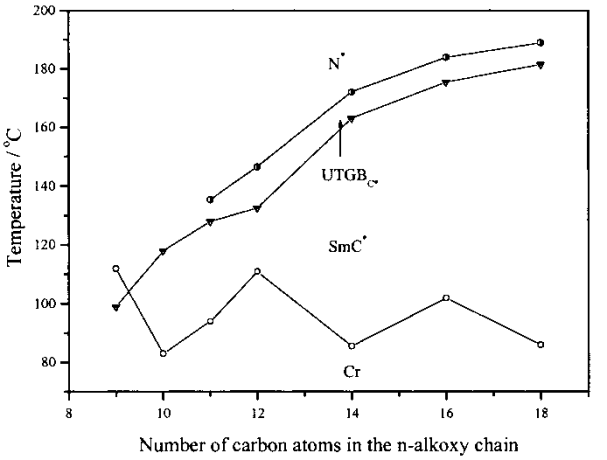

Figure 7. Plot of transition temperature *versus* the number of carbon atoms in the *n*-alkoxy chain for series II.

number of carbon atoms in the *n*-alkoxy chain for series II and III are shown in figures 7 and 8, respectively. The plots show general trends for like transitions. The SmC* to UTGB$_{C*}$ phase transition temperature increases on ascending the series. This rise is sharp for the lower homologues and appears to level off for the higher homologues. The overall thermal range of the UTGB$_{C*}$ phase varies from 1°C to 14°C.

3.2. *X-ray diffraction studies*

XRD studies were carried out on powder samples. The sample under investigation was filled into a 0.7 mm diameter Lindemann capillary tube in the cholesteric phase and sealed. The diffraction patterns were recorded on cooling the sample from the cholesteric phase to the SmC* phase. In the N* phase, a uniform ring with a rather broad radial intensity distribution was obtained. The real space periodicity, which produced this ring, was approximately equal to the total molecular length. On reducing the temperature to the UTGB$_{C*}$ phase, the ring became quite sharp when compared with that obtained for the N* phase for the same exposure time. The intense uniformly sharp ring obtained in the small angle region indicates a well organized layer structure, and a broad diffuse halo was observed in the wide angle region, which is characteristic of a fluid-like packing of the molecules. For compound **4**, the periodicity was calculated to be 34.8 Å, which is less than the total molecular length. This clearly indicates that the molecules are tilted with respect to the layer normal as in the case of a SmC* phase. The tilt angle was calculated to be 34°. On further cooling to the SmC* phase, a pattern similar to that observed for the UTGB$_{C*}$ phase was obtained. Hence, in a powder diffraction technique it is difficult to distinguish the SmC* and UTGB$_{C*}$ phases. These observations together with the Grandjean–Cano wedge experiments, where a square grid pattern with GC lines was obtained, confirms that this intermediate phase is indeed the UTGB$_{C*}$ phase. A plot of the intensity versus θ for the UTGB$_{C*}$ phase of compound **4** is shown in figure 9. The plot shows a well pronounced Bragg peak in the small angle region and a broad diffuse peak in the wide angle region, which indicates fluidity of the mesophase.

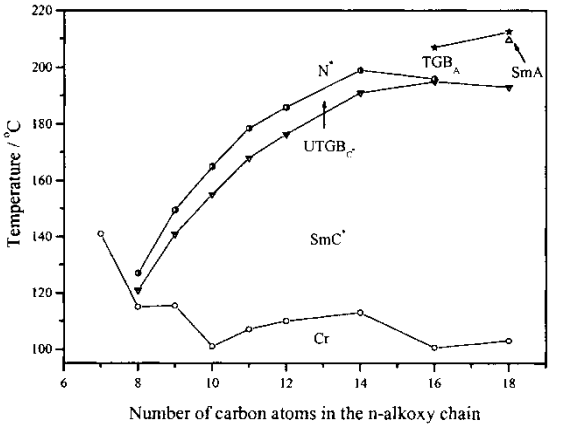

Figure 8. Plot of transition temperature *versus* the number of carbon atoms in the *n*-alkoxy chain for series III.

3.3. *Helical pitch measurements*

The helical pitch of the UTGB$_{C*}$ phase was measured using the standard Grandjean–Cano method [15, 16]. Thus, the sample was taken in a wedge-shaped cell of appropriate thickness (about 50 μm) and the spacing between the GC lines was measured as a function of temperature by cooling the sample from the cholesteric

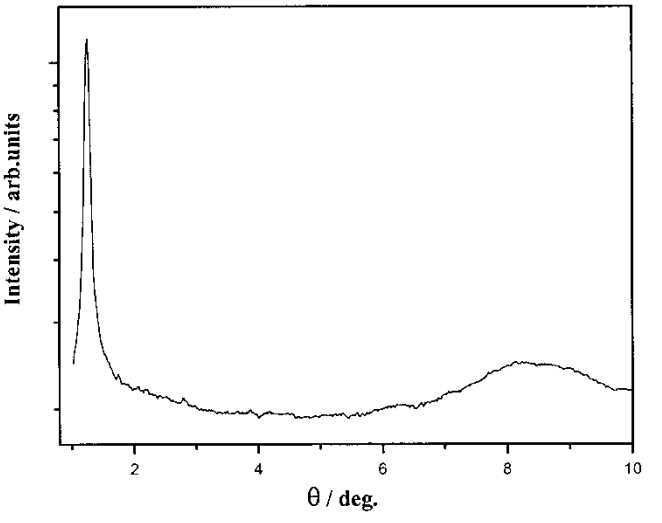

Figure 9. Plot of intensity *versus* θ for the UTGB$_{C*}$ phase of compound **4**.

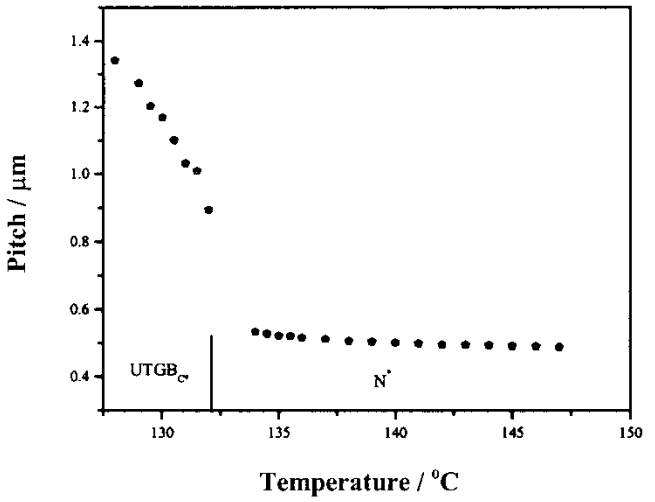

Figure 10. Plot of helical pitch versus temperature for compound **4**. The vertical line on the *X*-axis indicates the transition temperature.

phase at a slow rate of $0.2^{\circ}C\,min^{-1}$. The boundary conditions of the cell ensured that the helical axis of the sample was perpendicular to the glass plates. The plots of variation of pitch as a function of temperature for compounds **4**, **11** and **19** are shown in figures 10, 11 and 12, respectively. One can see from these plots that there is hardly any variation in the pitch length within the N* phase. However, at the N* $\rightarrow UTGB_{C*}$ phase transition, a significant jump in the pitch value can be seen. The magnitude of this jump varied depending on the nature of the compound. Therefore, a discontinuity in the slope can be seen at the transition point. On cooling further into the $UTGB_{C*}$ phase this value increased sharply. The variation of helical pitch with temperature

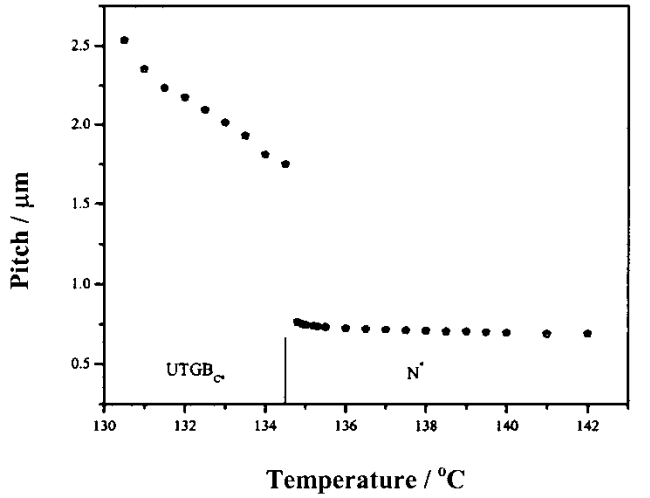

Figure 11. Plot of helical pitch versus temperature for compound **11**.

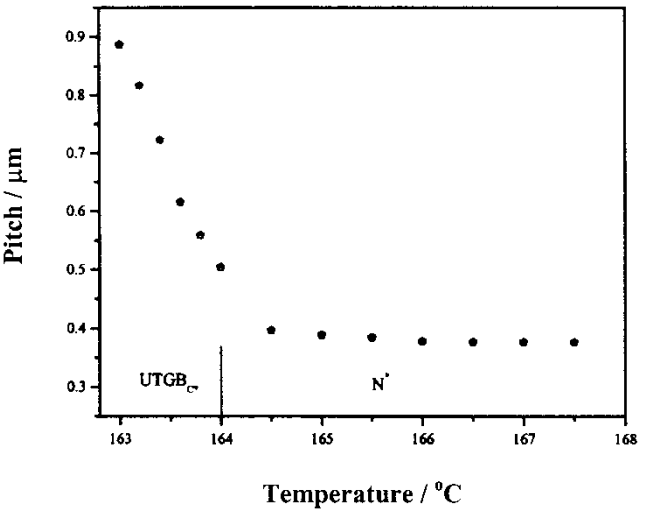

Figure 12. Plot of helical pitch versus temperature for compound **19**.

followed a trend similar to that observed for the mixture of compounds [8].

3.4. *Effect of lateral substitution*

The effect of lateral substitution on the core, especially a fluorine substituent, on the occurrence and stability of the $UTGB_{C*}$ phase has been examined. Consider the following two unsubstituted parent compounds **25** and **26**:

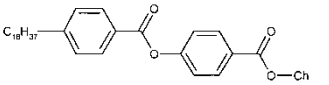

26

Cr 99.0 SmC* 165.0 SmA 200.5 TGB_A 205.0 N* >220 decomposes

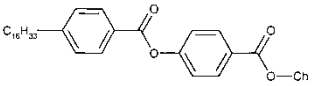

25

Cr 112.0 SmC* 175.0 SmA 200.0 TGB_A 200.0 N* >220 decomposes

Both these compounds exhibit N*, TGB_A, SmA and SmC* phases. Their mesomorphic properties can be compared with those of compounds **7** and **8** which exhibit N*, $UTGB_{C*}$ and SmC* phases at the expense of the SmA and the TGB_A phases as a result of the presence of the lateral fluorine substituent *ortho* to the carboxylate group close to the chiral moiety. This perhaps is due to the increase in the transverse moment adjacent to the chiral centre which favours the formation of tilted phases. Secondly, there is an increase in the molecular chirality brought about by the restricted rotation of the chiral moiety with respect

to the long molecular axis, due to the presence of the lateral fluoro substituent. A similar comparison can be made between the parent compounds **25** and **26** and those compounds **14** and **15** which contain an *n*-alkoxy chain. However, in the case of compounds **23** and **24**, there are two fluorine substituents and the phase behaviour is different. In compound **23**, a TGB_A phase exists between the $UTGB_{C*}$ and N* phases and the thermal range of the latter is reduced to only 1°C. Interestingly, on increasing the chain length, the $UTGB_{C*}$ phase is eliminated while retaining the four mesophases present in the parent compounds. If the position of the fluorine substituent is shifted to the *ortho* position with respect to the terminal *n*-alkoxy chain as in compound **27**, the $UTGB_{C*}$ phase is eliminated but TGB_A and SmA phases are induced;

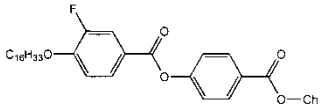

27

Cr 117.0 SmC^* 181.5 SmA 240.4 TGB_A 240.5 N^* >245 decomposes

The effect of the position of lateral fluoro substituents in compounds having two fluoro substituents can be illustrated by comparing the mesomorphic behaviour of compounds **23** and **28**.

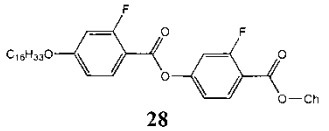

28

Cr 90.0 SmC^* 153.0 $UTGB_{C*}$ 160.5 N^* >220 decomposes

As can be seen in compound **28**, one of the fluorine substituents is *meta* to the terminal *n*-alkoxy chain and as a result, the TGB_A phase seen in compound **23** is eliminated while the thermal range of the $UTGB_{C*}$ phase increases from 1°C to 7.5°C. We have also examined two compounds **29** and **30** which contain a chloro or methoxy substituent, respectively, which is *ortho* to the terminal chain:

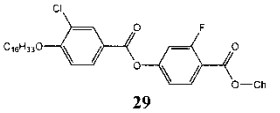

29

Cr 113.0 SmC^* 170.5 $UTGB_{C*}$ 183.0 N^* >240 decomposes

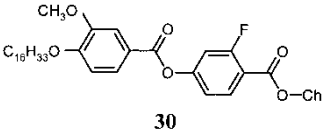

30

Cr 139.0 N^* 221.6 BP 221.8 I

In the case of compound **29**, the presence of a chloro substituent increases the thermal range of the $UTGB_{C*}$ phase from 1°C (compound **23**) to 12.5°C, while the TGB_A phase is completely suppressed. In contrast, when a bulky methoxy group is introduced (compound **30**), TGB_A, $UTGB_{C*}$ and SmC* phases are totally eliminated and only N* and blue phases can be observed. Hence, a combination of a chloro group *ortho* to the terminal *n*-alkoxy chain and a fluoro substituent *ortho* to the carboxylate group containing the chiral moiety favours not only the formation but also stabilizes the $UTGB_{C*}$ phase.

3.5. *Effect of the type of chiral moiety*

The type of chiral moiety present in the molecule is one of the prime factors for the occurrence of the twist grain boundary phases. In the compounds that we have studied, replacement of the cholesteryl moiety by a cholestanyl moiety has a significant effect. For example, compounds **31** and **32** have a cholestanyl moiety:

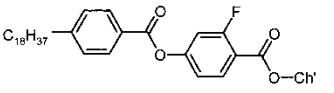

31

Cr 81.0 SmC^* 165.5 SmA 172.5 TGB_A179.5 N^* > 225 decomposes

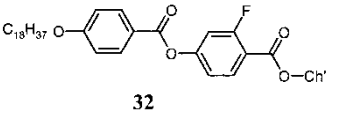

32

Cr 91.5 SmC^* 177.5 $UTGB_{C*}$ 180.5 N^* > 230 decomposes

Ch′= Cholestanyl moiety

The mesophases of these can be compared with those of compounds **8** and **15**, respectively. In compound **31** a $UTGB_{C*}$ phase was not observed but TGB_A and SmA phases were obtained. In compound **32** these two phases are replaced by the $UTGB_{C*}$ phase which is present in compounds **8** and **15**. This is perhaps due to the overall decrease in the polarity due to the reduction of the double bond present in the cholesteryl moiety. We have also examined compounds containing the [*S*]-[+]-octan-2-ol moiety as in compounds **33** and **34**. These are compounds containing four phenyl rings in the core, but as can be seen do not exhibit the $UTGB_{C*}$ phase. However, compound **33** shows a TGB_A phase, though over a very narrow range of temperature.

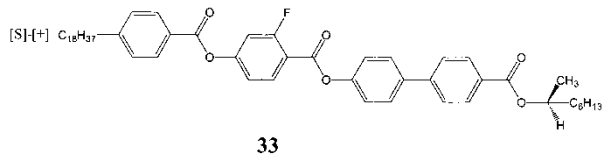

33

Cr 69.0 SmC* 156.5 SmA 165.9 TGB$_A$ 166.0 I

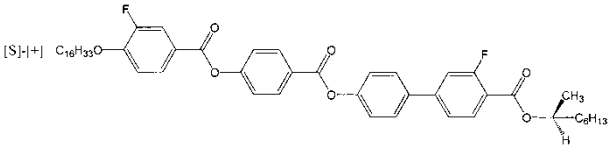

34

Cr 79.0 SmC* 201.0 SmA 215.0 I

From the above results, the following observations have been made. (i) In two-ring systems with cholesterol as the chiral moiety, the presence of a lateral fluorine substituent *ortho* to the carboxylate group and close to the chiral moiety is a prerequisite for the compounds to exhibit the UTGB$_{C*}$ phase. On the other hand, a lateral fluorine substituent *ortho* to the terminal *n*-alkoxy chain does not favour the formation of the UTGB$_{C*}$ phase. (ii) A sufficiently long alkyl/alkoxy chain ($n \geqslant 11$) is required for the monofluorine-substituted systems to exhibit this phase. (iii) In difluorine – substituted systems, the UTGB$_{C*}$ phase is destabilized in higher homologues ($n = 16$, 18). However, replacement of the fluorine *ortho* to the *n*-alkoxy chain by chlorine favours the formation of this phase, while a methoxy group destabilizes it. (iv). A difluorine-substituted system having a fluorine *meta* to the terminal chain stabilizes the occurrence of the UTGB$_{C*}$ phase. (v) Replacement of a cholesteryl group by a cholestanyl group as the chiral moiety does not favour the formation of the UTGB$_{C*}$ phase.

Since single component systems with groups other than cholesterol/cholestanol as the chiral moiety which exhibit this novel UTGB$_{C*}$ phase are not known, further work is necessary to determine the molecular structural requirements to obtain this interesting phase.

The authors would like to thank Mr K. Subrahmanya and Ms K.N. Vasudha for technical support and the Sophisticated Instruments Facility, Indian Institute of Science, Bangalore for the ^{1}H NMR spectra.

References

[1] Reinitzer, F., 1888, *Monatsh. Chem.*, **9,** 421.
[2] Meyer, R. B., Liebert, L., Strzelecki, L., and Keller, P., 1975, *J. Phys. Lett.*, **36,** L–69.
[3] Chandani, A. D. L., Gorecka, E., Ouchi, Y., Takezoe, H., and Fukuda, A., 1989, *Jpn. J. appl. Phys.*, **28,** L1265.
[4] Renn, S. R., and Lubensky, T. C., 1988, *Phys. Rev. A*, **38,** 2132.
[5] Goodby, J. W., Waugh, M. A., Stein, S. M., Chin, E., Pindak, R., and Patel, J. S., 1989, *Nature*, **337,** 449.
[6] Goodby, J. W., Waugh, M. A., Stein, S. M., Chin, E., Pindak, R., and Patel, J. S., 1989, *J. Am. chem. Soc.*, **111,** 8119.
[7] Renn, S. R., 1992, *Phys. Rev. A.*, **45,** 953.
[8] Pramod, P. A., Pratibha, R., and Madhusudana, N. V., 1997, *Curr. Sci.*, **73,** 761.
[9] Sadashiva, B. K., 1999, *Pramana*, **53,** 213.
[10] Gray, G. W., and Jones, B., 1953, *J. chem. Soc.*, 4179.
[11] Weigand, C., and Gabler, R., 1940, *Z. phys. Chem.*, **1346,** 270.
[12] Gray, G. W., and Jones, B., 1954, *J. chem. Soc.*, 2556.
[13] Gray, G. W., Hogg, C., and Lacey, D., 1981, *Mol. Cryst. liq. Cryst.*, **67,** 1.
[14] Kasthuraiah, N., Sadashiva, B. K., Krishnaprasad, S, and Nair, G. G., 1998, *Liq. Cryst.*, **24,** 639.
[15] Grandjean, F., 1922, *C.R. Acad. Sci., Paris*, **172,** 71.
[16] Bouligand, Y., 1974, *J. Phys.*, **35,** 958.
[17] Gorecka, E., Glogarova, M., Sverenyak, H., and Lejeck, L., 1996, *Ferroelectrics*, **178,** 101.
[18] Langer, S. A., and Sethna, J. P., 1986, *Phys. Rev. A.*, **34,** 5035.
[19] Hinshaw, G. A., and Petschek, R. G., 1988, *Phys. Rev. Lett.*, **60,** 1988.
[20] Hinshaw, G. A., and Petschek, R. G., 1989, *Phys. Rev. A.*, **39,** 5914.